LA-11504-MS
UC-
Issued: February 1989

LA--11504-MS
DE89 007100

Fracture-Coating Minerals in the Topopah Spring Member and Upper Tuff of Calico Hills from Drill Hole J-13

Barbara Carlos

Los Alamos National Laboratory
Los Alamos, New Mexico 87545

FRACTURE-COATING MINERALS IN THE TOPOPAH SPRING MEMBER AND UPPER TUFF OF CALICO HILLS FROM DRILL HOLE J-13

by

Barbara Carlos

ABSTRACT

Fracture-lining minerals from drill core in the Topopah Spring Member of the Paintbrush Tuff and the tuff of Calico Hills from water well J-13 were studied to identify the differences between these minerals and those seen in drill core USW G-4. In USW G-4 the static water level (SWL) occurs below the tuff of Calico Hills, but in J-13 the water table is fairly high in the Topopah Spring Member. There are some significant differences in fracture minerals between these two holes. In USW G-4 mordenite is a common fracture-lining mineral in the Topopah Spring Member, increasing in abundance with depth. Euhedral heulandite >0.1 mm in length occurs in fractures for about 20 m above the lower vitrophyre. In J-13, where the same stratigraphic intervals are below the water table, mordenite is uncommon and euhedral heulandite is not seen. The most abundant fracture coating in the Topopah Spring Member in J-13 is drusy quartz, which is totally absent in this interval in USW G-4. Though similar in appearance, the coatings in the vitrophyre have different mineralogy in the two holes. In USW G-4 the coatings are extremely fine grained heulandite and smectite. In J-13 the coatings are fine-grained heulandite, chabazite, and alkali feldspar. Chabazite has not been identified from any other hole in the Yucca Mountain area. Fractures in the tuff of Calico Hills have similar coatings in core from both holes. In J-13, as in USW G-4, the tuff matrix of the Topopah Spring Member is welded and devitrified and that of the tuff of Calico Hills is zeolitic. The comparison of fracture coatings in J-13 and USW G-4 suggests that zeolites are not stable on fracture surfaces in nonzeolitic tuffs below the water table. Zeolites may have formed on fractures in the densely welded devitrified tuffs of the Topopah Spring Member but dissolved upon submersion below the water table. Alternatively, zeolites may have been inhibited from crystallizing on fracture surfaces in J-13 because the Topopah Spring Member became partially submerged beneath the water table soon after deposition.

I. INTRODUCTION

Water well J-13 was begun in 1962 and completed in January 1963 by the U.S. Geological Survey (USGS) near Fortymile Wash in Jackass Flats (Fig. 1). The well was originally identified as test well 6, but was redesignated J-13 when it became a producing water well. Static water level (SWL) was at 927 ft depth after completion in 1963 (Young, 1972). Approximately 10% core was taken; the rest of the hole was sampled by drill bit cuttings collected every 5 or 10 ft. The cored intervals are shown in Fig. 2. Although the well was drilled before the DOE Yucca Mountain Project (YMP), most of the water used in water-rock reaction tests for YMP comes from this well because it is near Yucca Mountain and the producing unit is the Topopah Spring Member of the Paintbrush Tuff.

The drilling history of the well and a partial lithologic description are given by Doyle and Meyer (1963). Young (1972) discusses the hydrology of Jackass Flat and the wells in it. Heiken and Bevier (1979) describe the petrology of the tuff based on core samples, with emphasis on the original volcanic textures and the zonation of alteration minerals with depth. Little information is given on fracture minerals. Bish and Chipera (1986) reanalyzed all the original whole rock powder samples of Heiken and Bevier, using quantitative x-ray diffraction (XRD). Table I contains the data from their Table II for the interval of interest to this study. Byers and Warren (1983) present a revised stratigraphy of the drill hole, with emphasis on the lower units, which had not been well studied at the time of the earlier reports. Broxton et al. (1986) include some data on J-13 samples along with data from other holes and outcrops in their discussion of the chemistry of altered tuffs at Yucca Mountain, and Bish et al. (1982) include J-13 in their discussion of the tuffs of Yucca Mountain.

Interest in the fracture mineralogy of J-13 was kindled by discussions of what would happen to the fracture-lining minerals seen in USW G-4 should the lower Topopah Spring Member become saturated. On Yucca Mountain the SWL occurs below the Paintbrush Tuff and most of the tuff of Calico Hills. In well J-13 the water table is fairly high in the Topopah Spring Member (Fig. 2); therefore the fracture mineralogy of J-13 provides an interesting comparison with that of USW G-4. Because the interval of interest is only that which is above the water table in USW G-4, only samples from the Topopah Spring Member and the tuff of Calico Hills were examined. Two samples in this interval from Heiken and Bevier's study contained fractures and were included in this study. D. Broxton provided cuttings samples used in his report. Core was examined and additional samples

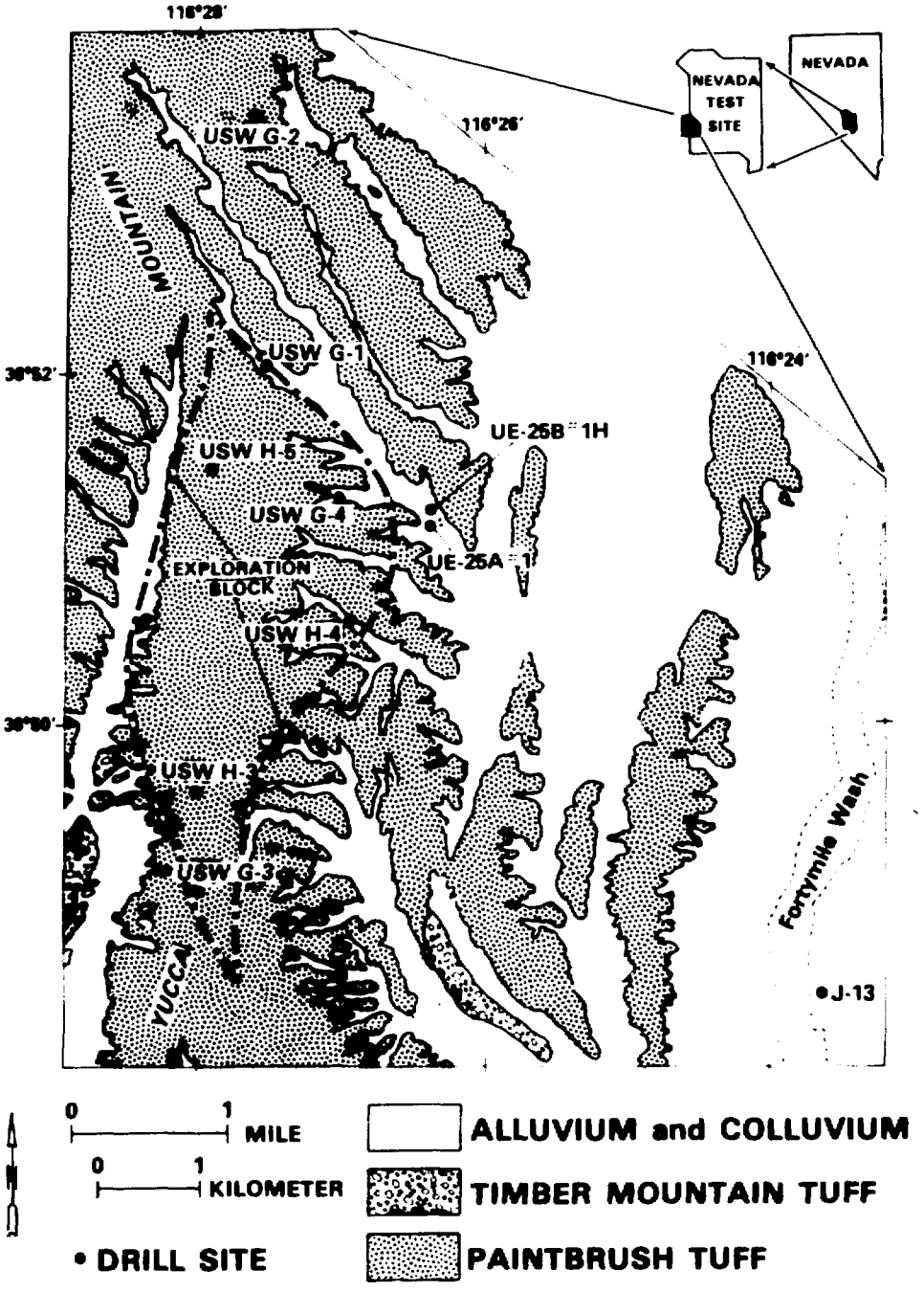

Fig. 1.
Location map showing Yucca Mountain and drill holes.

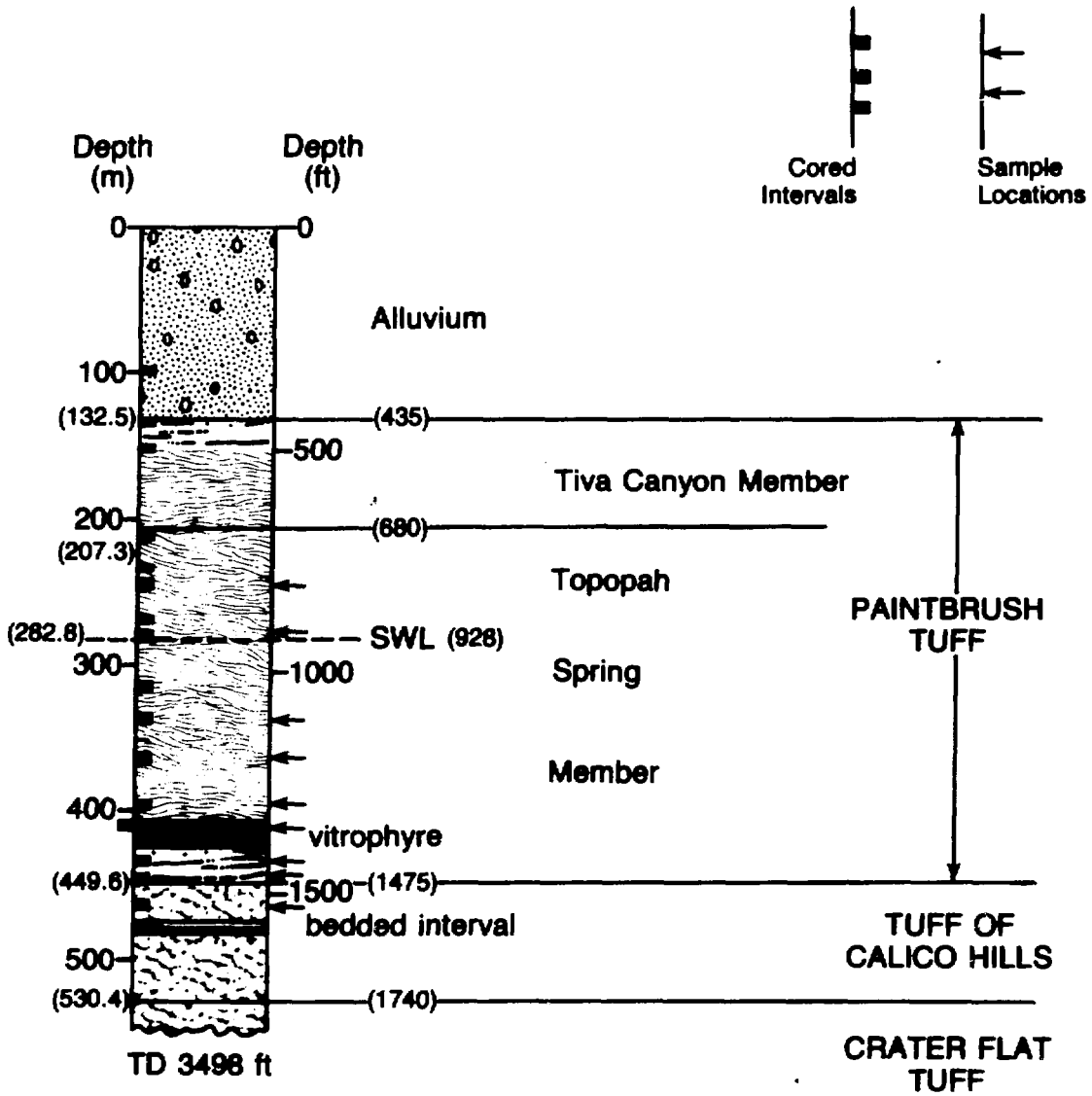

Fig. 2.
Graphic log of upper 1800 ft of well J-13 showing cored intervals and sample depths; density of pattern is roughly proportional to density of welding. Modified from Byers and Warren, 1983.

TABLE I

X-RAY DIFFRACTION ANALYSES OF TUFF FROM DRILL HOLE J-13 (weight percent)
(data from Bish and Chipera, 1986)

Sample[a]	Depth (m)	Method[b]	Smectite	Mica	Clino-ptilolite	Morden-ite	Anal-cime	Quartz	Tridy-mite	Cristo-balite	Opal-CT	Glass	Alkali Feldspar	Calcite	Hematite
Topopah Spring Member															
J13-689	210.0	E	26±5		1±1			5±1		13±1			54±6		Tr
J13-801	244.1	I	2±1					1±1	6±1	23±1			66±10		Tr
J13-925	281.9	I	3±1	Tr				29±1	2±1	3±1			62±8		
Static Water Level															
J13-1033	314.9	I	1±1	Tr				30±1	2±1				69±9		Tr
J13-1102	335.9	I	Tr	Tr				20±1	2±1				78±10		Tr
J13-1194	364.0	E		Tr				33±1					67±8		Tr
J13-1292	394.0	I		Tr				33±1					63±7		Tr
J13-1296	395.0	E						36±1					64±8		Tr
J13-1345	410.0	I						Tr			11±2	81±3	8±1		
J13-1421	433.0	E	3±1	Tr	27±3			Tr			25±5	30±15	13±2		
J13-1457	444.1	I	2±1		80±8			2±1			8±2		7±1	Tr	
Tuff of Calico Hills															
J13-1512	460.9	I	Tr		47±12			5±1			39±8		6±1		
J13-1515	462.0	I	4±1		64±6			1±1			12±2		14±3		
J13-1519	463.0	I	5±1		56±8	Tr		7±1			18±4		13±2		

[a]Sample designation, e.g., J13-427 refers to a sample from drill hole J-13 at 427 ft depth.

[b]I = Internal Standard Method; E = External Standard Method.

TABLE II

X-RAY DIFFRACTION ANALYSES OF FRACTURE-LINING MINERALS FROM DRILL HOLE J-13

Sample	Smectite	Heulandite-Clinoptilolite	Mordenite	Quartz	Tridymite	Cristobalite Opal-C	Alkali Feldspar	Other
J-13 800 B	x			x	x		x	
J-13 1101 A				x			x	a
J-13 1102				x				
J-13 1345	Tr	x				x	x	b
J-13 1456	Tr?	x	Tr			x		
J-13 1519		x	x	x				

[a]Lithiophorite(?).

[b]Chabazite.

were collected from all the core (except the vitrophyre, for which the original samples were sufficient) in the interval of interest (762 to 1580 ft). Cuttings were examined from an interval of approximately 80 ft above the vitrophyre, but no additional samples were taken.

II. METHODS

Samples were analyzed using a combination of methods including examination by both binocular and petrographic microscope, scanning electron microscope (SEM) imaging and qualitative element analysis, XRD analysis, and microprobe analysis of thin sections. These methods are described in greater detail in Carlos (1985, 1987). The qualitative results of the XRD analyses are given in Table II. Because of limitations imposed by the small amounts of material available, no attempt has been made to quantify these results.

III. FRACTURE LININGS IN THE TOPOPAH SPRING MEMBER

A. Above the Vitrophyre

Three core samples were taken from the part of the Topopah Spring Member above the SWL in well J-13. The most abundant fracture coating is that described as

"lithophysal-type" in USW G-4 (Carlos 1985). These fractures are characterized by a bleached zone in the matrix surrounding the fracture and a preponderance of silica minerals in the fracture. In the sample from 800 ft depth, the silica minerals are predominantly euhedral tridymite, with minor quartz, probably as overgrowths on the tridymite (Fig. 3). Minor phases include smectite and alkali feldspar, which may have been in the bleached zone rather than the fracture itself, and a trace of iron oxide mineral on the surface of the fracture between the tridymite crystals.

A second, much less frequent, fracture coating from the same cored interval consists of small crusts of fine-grained zeolite, most likely mordenite, with a maximum fiber length of about 10 μm. Large amounts of silica in some of the mordenite(?) crusts suggest that cristobalite may be intergrown with the zeolite. Manganese oxides occur as small lobate spots in amounts too small for analysis by XRD. SEM imaging revealed interlocking clusters of radiating bristles 1 to 2 μm long forming the lobes (Fig. 4). Qualitative element analysis of these bristles indicated a composition of Mn with minor Ca and Si. The Si may be substrate, but the Ca must be in the manganese oxide itself as the value is too high for substrate. Based on its major element chemistry and crystal form, the Mn oxide is suspected to be todorokite.

A third fracture coating occurs on most fractures in the core just above the water table. This coating consists entirely of manganese spots, which in some fractures become nearly continuous. The coating is very thin, however, and insufficient material was available for XRD analysis. The manganese oxide is extremely fine grained, and the morphology of individual crystals on the sample from 924 ft could not be resolved on SEM images at 5000x magnification. The qualitative chemistry obtained on the SEM identifies Si, Ce, Ba, and Ca as the most abundant elements after manganese. Minor constituents include K, Fe, and Mg.

In the Topopah Spring Member between the water table and the vitrophyre, the predominant fracture coating is etched or partially dissolved euhedral quartz, often with small protrusions of anhedral or, more rarely, globular silica overgrowths (Figs. 5, 6). Manganese oxide mineral(s) commonly occurs with the quartz. At 1101 ft the manganese oxide mineral forms small (<1-μm diameter) nearly hexagonal plates and occurs beneath the quartz (Fig. 7). The XRD pattern is compatible with either todorokite or lithiophorite; the form suggests lithiophorite, and the chemistry, as obtained from the SEM, includes (in addition to Mn) Ca, Al, Ba, Si, Zn, Cu, Fe, and K. At 1194 ft depth the manganese oxide

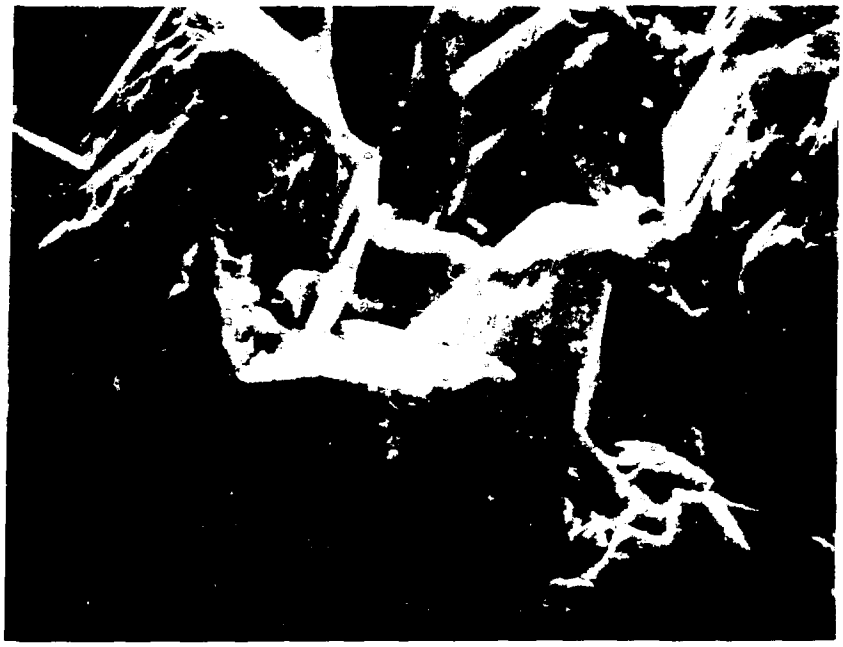

Fig. 3.
Tridymite with silica overgrowths in lithophysal-type fracture from 800 ft (above water table).

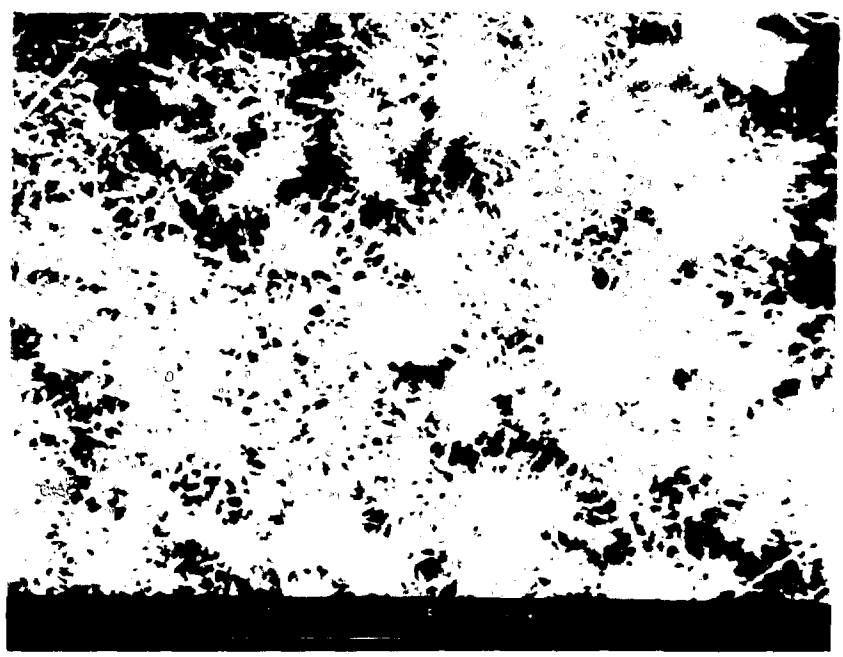

Fig. 4.
Detail of lobate manganese oxide from 800 ft.

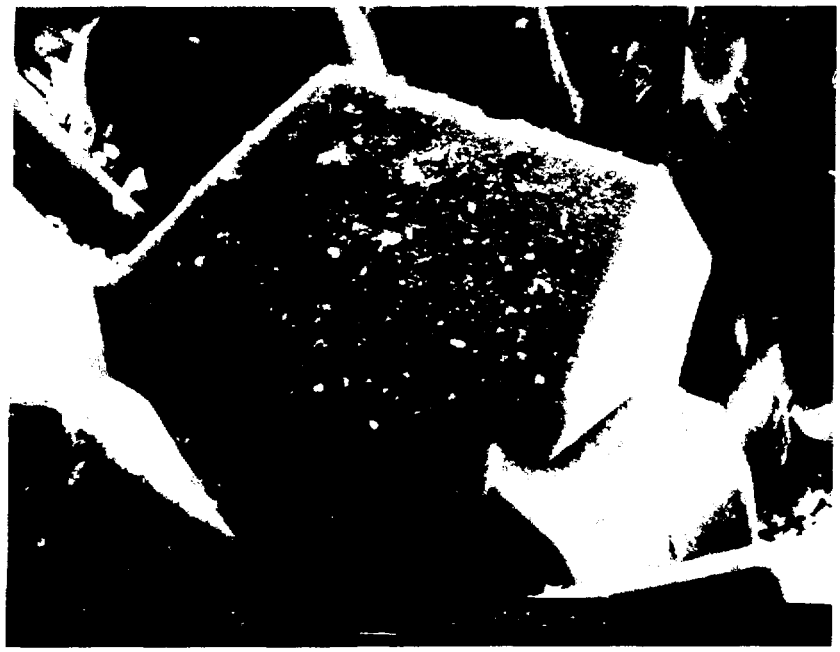

Fig. 5.
Silica overgrowths on etched euhedral quartz from 1194 ft.

Fig. 6.
Silica overgrowths (some globular) on etched euhedral quartz from 1292 ft.

mineral(s) associated with the quartz occurs as both plates and fibers and appears to have a somewhat simpler chemistry: Mn, Ca, Si, K, Al, and Ti. Sparse mordenite (?) can be seen on the manganese in the SEM images of the sample from 1101 ft (Fig. 7), and on quartz at 1102 ft (Fig. 8), but it occurs in amounts too small to be seen in the XRD pattern. No calcite was found in any of the fractures in J-13.

Lithophysal-type coatings were observed in only one core in this interval. Carlos (1985) noted in USW G-4 that the lithophysal coatings were closely related to lithophysal zones in the tuff and less abundant in nonlithophysal zones. It is expected that the same relationship exists in this hole, and since the coring was intermittent, the apparent sparsity of lithophysal-type fractures may not be representative. The lithophysal-type coating sampled at 1102 ft is pure quartz, determined by XRD analysis. SEM images indicate that the quartz is pseudomorph after tridymite and is overgrown with trace amounts of a fibrous mineral, probably mordenite (Fig. 8).

Cuttings were examined from the intervals 1240-1270 ft and 1300-1330 ft to determine the fracture mineralogy of these important uncored intervals. Because these cuttings could be examined only at 10x magnification, very thin fractures will go undetected. The only fracture-coating mineral identified in the cuttings was euhedral quartz. Euhedral heulandite, so abundant in the interval above the vitrophyre in USW G-4, was not observed.

B. Vitrophyre

Fractures in the vitrophyre contain cryptocrystalline white and orange coatings that closely resemble those seen in USW G-4. The minerals identifiable by XRD from the sample at 1345 ft depth are chabazite, heulandite, and minor alkali feldspar. This is the first chabazite identified near Yucca Mountain. Cristobalite is not present. Manganese oxide occurs as plates embedded in the coating. The chemistry of the manganese oxide as determined by electron microprobe is given in Table III. It is similar to the qualitative analysis obtained by SEM on the sample at 1101 ft, but the mineral has not yet been identified. Thin sections were made across two of the fractures in the core from 1345 ft. The coating in one was silica and manganese oxide, and the other contained zeolite(s). The analysis of the coarser grained zeolite in this sample is given in Table IV; the chemistry could be that of chabazite or heulandite. The analyses are plotted with clinoptilolites on Fig. 9 for comparative purposes.

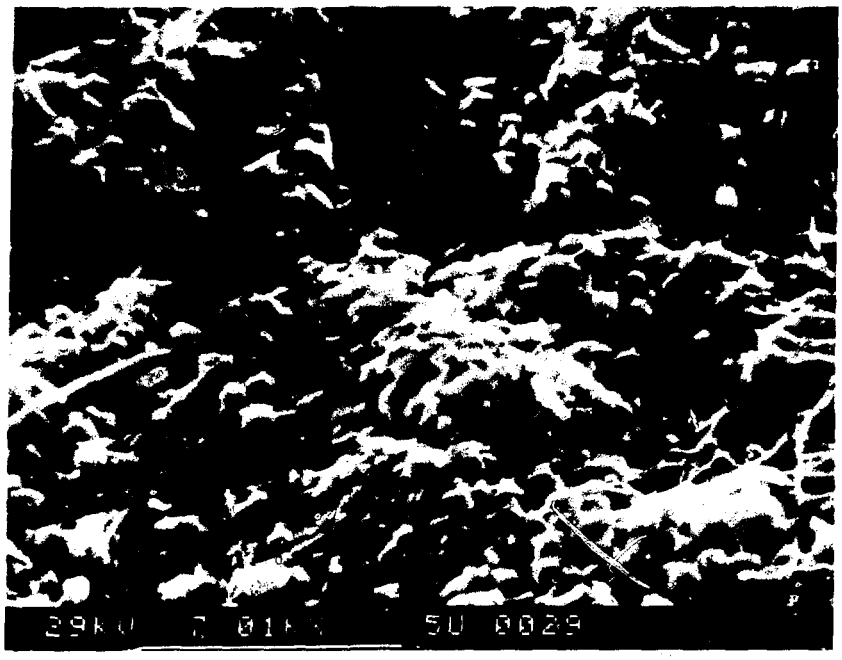

Fig. 7.
Hexagonal plates of manganese oxide mineral with fibers of mordenite from 1101 ft.

Fig. 8.
Quartz after tridymite in lithophysal-type fracture from 1102 ft. Fibers on surface are probably mordenite.

TABLE III

MN OXIDE MINERAL(S) FROM FRACTURE AT 1345 FT DEPTH[a]

SiO_2	2.63	4.46	4.19	3.01	2.22	5.88	5.30	2.14	2.61
TiO_2	-	-	0.13	0.69	0.56	-	-	-	0.23
MnO_2	81.42	73.75	73.86	76.81	83.02	70.88	74.04	80.74	79.95
CeO_2	-	0.41	0.32	0.34	-	0.67	0.39	-	0.52
Al_2O_3	0.74	0.94	0.97	1.11	1.08	1.20	1.25	0.89	0.50
Fe_2O_3	0.21	0.69	0.57	0.99	0.66	0.42	0.17	0.35	0.75
MgO	0.05	0.14	0.18	0.06	-	0.05	-	0.17	0.06
CaO	1.62	3.38	3.32	1.46	1.06	1.67	1.36	1.14	1.25
SrO	0.49	0.48	0.42	0.48	0.38	0.58	0.57	0.34	0.44
BaO	2.82	2.78	2.86	2.00	1.56	3.21	2.81	1.46	2.35
PbO	0.64	0.66	0.55	0.81	0.68	1.31	1.31	0.58	2.21
Na_2O	0.94	1.34	1.35	0.99	0.65	0.74	0.71	0.92	0.69
K_2O	3.54	0.91	1.28	2.98	4.81	2.23	3.28	3.21	4.09
La_2O_3	0.13	-	0.16	-	-	0.15	0.21	-	0.10
Total[b]	95.23	89.94	90.16	91.73	96.68	88.99	91.40	91.94	95.75
Si^{+4}	0.33	0.59	0.55	0.39	0.28	0.79	0.70	0.28	0.33
Ti^{+4}	-	-	0.01	0.07	0.05	-	-	-	0.02
Mn^{+4}	7.15	6.75	6.76	6.94	7.14	6.60	6.72	7.25	7.09
Ce^{+4}	-	0.02	0.01	0.02	-	0.03	0.02	-	0.02
Al^{+3}	0.11	0.15	0.15	0.17	0.16	0.19	0.19	0.14	0.08
Fe^{+3}	0.02	0.07	0.06	0.10	0.06	0.04	0.02	0.03	0.07
Mg^{+2}	0.01	0.03	0.04	0.01	-	0.01	-	0.03	0.01
Ca^{+2}	0.22	0.48	0.47	0.20	0.14	0.24	0.19	0.16	0.17
Sr^{+2}	0.04	0.04	0.03	0.04	0.03	0.05	0.04	0.03	0.03
Ba^{+2}	0.14	0.14	0.15	0.10	0.08	0.17	0.14	0.07	0.12
Pb^{+2}	0.02	0.02	0.02	0.03	0.02	0.05	0.05	0.02	0.08
Na^{+1}	0.23	0.34	0.35	0.25	0.16	0.19	0.18	0.23	0.17
K^{+1}	0.57	0.15	0.22	0.50	0.76	0.38	0.55	0.53	0.67
La^{+3}	0.01	-	0.01	-	-	0.01	0.01	-	0.00
TOTAL	8.85	8.78	8.83	8.82	8.88	8.75	8.82	8.77	8.87
Oxygen	16.00	16.00	16.00	16.00	16.00	16.00	16.00	16.00	16.00

[a]Elements included in the analyses but not detected are Co, Ni, Cu, Zn, and P. No additional elements were observed by energy dispersive analysis.

[b]Low totals are at least partially the result of H_2O not included in analysis.

TABLE IV

COMPOSITIONS OF ZEOLITES AT 1345 ft DEPTH IN DRILL HOLE J-13

SiO_2	63.6	62.7	62.4	60.6	64.1	62.3	63.8	63.9
TiO_2	0.00	0.04	0.00	0.00	0.00	0.00	0.00	0.00
Al_2O_3	14.9	14.8	14.4	14.4	14.7	14.9	15.0	15.1
Fe_2O_3	0.02	0.00	0.03	0.00	0.00	0.00	0.00	0.00
MgO	0.00	0.00	0.00	0.00	0.00	0.00	0.00	0.00
CaO	5.33	5.19	5.24	5.30	5.38	5.28	4.91	5.06
BaO	0.07	0.03	0.00	0.03	0.04	0.05	0.00	0.08
Na_2O	0.61	0.66	0.83	0.51	0.43	0.66	0.86	0.67
K_2O	4.09	4.13	4.54	3.63	2.76	3.92	4.49	3.51
TOTAL	88.6	87.6	87.5	84.5	87.4	87.0	89.0	88.3
Unit-Cell Composition Based on 72 (O)								
Si	28.2	28.1	28.1	28.1	28.5	28.1	28.2	28.3
Ti	0.00	0.01	0.00	0.00	0.00	0.00	0.00	0.00
Al	7.76	7.82	7.68	7.90	7.69	7.90	7.82	7.87
Fe	0.01	0.00	0.01	0.00	0.00	0.00	0.00	0.00
Mg	0.00	0.00	0.00	0.00	0.00	0.00	0.00	0.00
Ca	2.53	2.49	2.53	2.63	2.56	2.55	2.32	2.40
Ba	0.01	0.01	0.00	0.01	0.01	0.01	0.00	0.01
Na	0.52	0.57	0.73	0.46	0.37	0.58	0.74	0.57
K	2.31	2.36	2.61	2.15	1.56	2.26	2.53	1.98
Si/(Al+Fe)	3.63	3.60	3.66	3.56	3.70	3.56	3.60	3.59
(Al+Fe)/(2Mg+2Ca+2Ba+Na+K)	0.98	0.99	0.91	1.00	1.09	0.99	0.99	1.07
Mol.% Exchangeable Cations								
K	43.1	43.5	44.5	41.0	34.8	41.9	45.3	40.0
Na	9.8	10.6	12.4	8.8	8.2	10.7	13.2	11.6
Ca+Mg	47.2	45.9	43.1	50.3	57.0	47.4	41.6	48.4

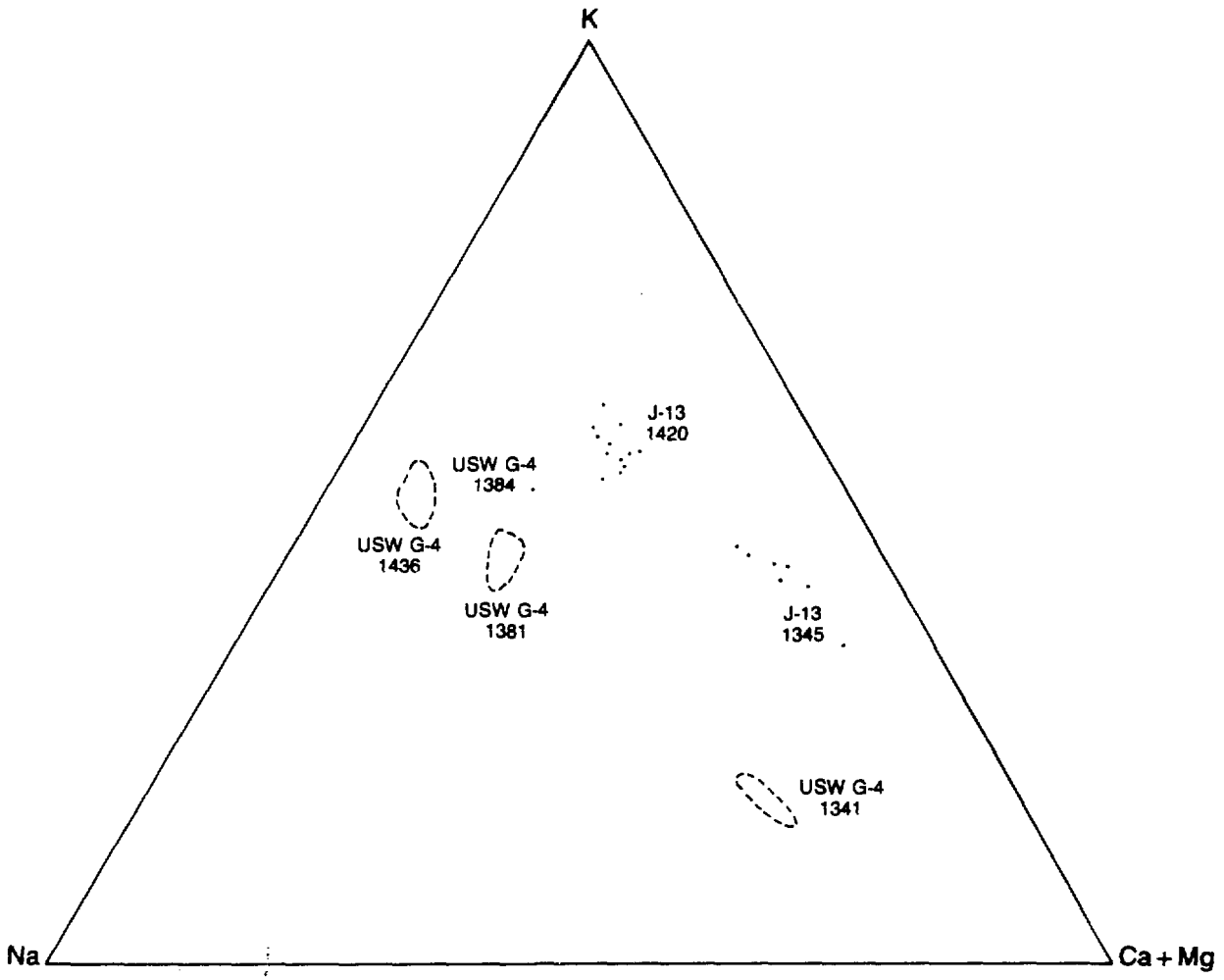

Fig. 9.
Fracture-lining clinoptilolites in USW G-4 and J-13.

D. Broxton provided thin sections of the drill bit cuttings for which clinoptilolite analyses were reported in Broxton et al. (1986). All of the fractures in these samples were determined by SEM to contain pure silica. The clinoptilolite reported by Broxton et al. occurs in altered shards rather than fractures.

C. Below the Vitrophyre

Two samples were taken from the Topopah Spring Member below the vitrophyre. In neither sample could the coating be identified visually, but both appear to be primarily extremely fine grained (<1-μm) clinoptilolite. The coating at 1420 ft depth is on a closed fracture that was thin-sectioned for microprobe analysis. The fracture mineral occurs as

plumose or radiating crystallites, but the chemistry suggests clinoptilolite rather than mordenite (Table V, Fig. 9). The sample at 1456 ft contained many bristly fibers about 5 μm in length held together by a smooth interstitial material. The minerals in this sample were identified by XRD as clinoptilolite, cristobalite (opal-C?), and traces of mordenite and possibly smectite.

IV. FRACTURE COATINGS IN THE TUFF OF CALICO HILLS

The single sample taken from the Calico Hills at 1520 ft depth has a fracture coating of clinoptilolite, mordenite, and minor quartz. The mordenite is clearly identifiable in SEM images by its fibrous habit; the tiny blocky grains (1-3 μm) embedded in the mordenite are believed to be clinoptilolite (Fig. 10). Only one core from the Calico Hills was available for sampling. The second core indicated on Fig. 2 was taken in a nonindurated bedded interval and has disaggregated.

V. COMPARISON TO USW G-4

An important limiting factor in this study is the lack of continuous core in J-13, particularly in the interval immediately above the vitrophyre. Fracture minerals are poorly preserved in drill bit cuttings, the dominant sample type available for this hole. Despite the limited samples available for study in J-13, this study revealed significant differences between the fracture minerals in the J-13 hole and those in USW G-4.

Though tridymite is preserved in lithophysal fractures above the water table in J-13, below the water table it has been replaced by quartz. Some tridymite is also preserved in lithophysal fractures in USW G-4. The most abundant fracture coating in the Topopah Spring Member below the water table in J-13 is euhedral quartz in nonlithophysal-type fractures. In USW G-4 quartz is rare in nonlithophysal fractures, which are characterized by patchy mordenite and traces of manganese oxide minerals. A trace of mordenite was seen in one interval below the water table in J-13, but it is much less abundant than in USW G-4. In USW G-4 a thin layer containing heulandite-clinoptilolite occurs just above the basal vitrophyre of the Topopah Spring Member (Bish and Vaniman, 1985). An interval of abundant euhedral (>0.1-mm-length) heulandite in the fractures begins about 50 ft above this zeolitic zone (Carlos, 1985). Neither zeolitic matrix nor vein heulandite is seen in J-13. It is possible that the cored interval at 1291-1296 ft is just above such a

TABLE V

COMPOSITIONS OF CLINOPTILOLITES AT 1420 ft DEPTH IN DRILL HOLE J-13

SiO_2	65.3	64.9	66.8	66.7	67.2	66.0	68.2	68.0
TiO_2	0.00	0.00	0.01	0.01	0.00	0.01	0.00	0.00
Al_2O_3	12.2	12.3	11.9	12.2	12.4	12.5	12.3	12.4
Fe_2O_3	0.03	0.00	0.11	0.00	0.03	0.04	0.06	0.00
MgO	0.00	0.00	0.00	0.00	0.00	0.00	0.00	0.00
CaO	2.51	2.46	2.52	2.59	2.61	2.51	2.46	2.55
BaO	0.00	0.00	0.00	0.00	0.00	0.00	0.00	0.00
Na_2O	1.31	1.26	1.24	1.10	1.08	1.18	1.14	1.17
K_2O	5.68	5.35	4.50	4.43	4.55	5.97	4.71	4.86
TOTAL	87.0	86.3	87.1	87.0	87.9	88.2	88.9	89.0
Unit-Cell Composition Based on 72 (O)								
Si	29.4	29.4	29.8	29.7	29.7	29.4	29.8	29.7
Ti	0.00	0.00	0.00	0.00	0.00	0.00	0.00	0.00
Al	6.48	6.58	6.26	6.39	6.45	6.55	6.31	6.39
Fe	0.01	0.00	0.04	0.00	0.01	0.01	0.02	0.00
Mg	0.00	0.00	0.00	0.00	0.00	0.00	0.00	0.00
Ca	1.21	1.19	1.20	1.24	1.23	1.20	1.15	1.19
Ba	0.00	0.00	0.00	0.00	0.00	0.00	0.00	0.00
Na	1.15	1.11	1.07	0.95	0.92	1.02	0.96	0.99
K	3.27	3.09	2.56	2.52	2.56	3.39	2.62	2.71
Si/(Al+Fe)	4.54	4.47	4.72	4.65	4.59	4.48	4.71	4.64
(Al+Fe)/(2Mg+2Ca+2Ba+Na+K)	0.95	1.00	1.04	1.08	1.09	0.96	1.07	1.05
Mol.% Exchangeable Cations								
K	58.1	57.3	52.9	53.5	54.3	60.5	55.4	55.4
Na	20.4	20.5	22.2	20.2	19.6	18.2	20.4	20.3
Ca+Mg	21.6	22.1	24.9	26.3	26.1	21.4	24.3	24.4

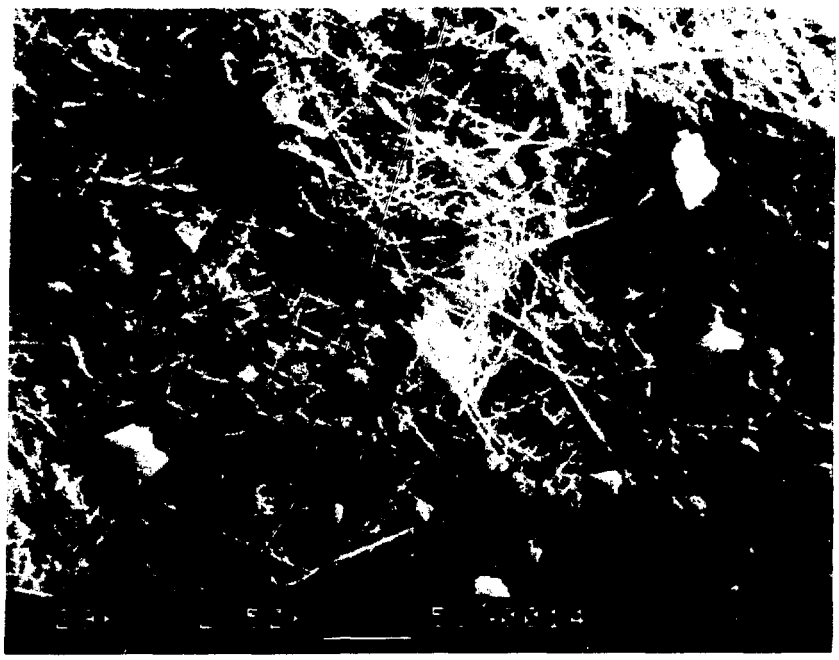

Fig. 10.
Mordenite and clinoptilolite from fracture at 1520 ft.

zeolitic interval, but if the fracture mineralogy were similar to that of USW G-4, the fractures would contain visible heulandite. Neither core nor cuttings above the vitrophyre in J-13 contain identifiable heulandite. However, drusy quartz is abundant.

The fracture coatings in the vitrophyre in USW G-4 and in J-13 are cryptocrystalline white and orange colored with spots of an unidentified manganese oxide. In J-13 the coatings are heulandite or clinoptilolite, chabazite, and minor alkali feldspar. This is the first identification of chabazite in the Yucca Mountain area. In USW G-4 the coatings are heulandite and smectite. Fracture coatings in the vitrophyre of both drill holes are too fine grained to determine crystal morphology even in SEM images at 6000x magnification. However, the XRD patterns show the material in J-13 is much better crystallized than that in USW G-4, which gives broad, ill-defined peaks.

Below the vitrophyre in the Topopah Spring Member in J-13 both the tuff matrix and the fractures contain zeolites, primarily clinoptilolite, though glass shards are well preserved inside alteration rims. There is no nonzeolitic nonwelded interval below the vitrophyre as there is in USW G-4, where it is above the water table.

The fracture coating in the tuff of Calico Hills resembles that in USW G-4. The tuff matrix in both holes is mostly clinoptilolite, but the most visible fracture coating is mordenite. The clinoptilolite seen in the XRD patterns of fracture coatings in both holes is probably the small, mostly anhedral grains embedded in the mordenite.

VI. DISCUSSION

Several differences were observed between the fracture minerals of USW G-4 and those of J-13: near absence of mordenite in the Topopah Spring Member in J-13, absence of coarse-grained heulandite and abundance of drusy quartz in fractures in the interval above the lower vitrophyre in J-13, and the presence of chabazite with heulandite in fractures in the vitrophyre.

Mordenite-coated fractures are common in the densely welded devitrified tuff of the Topopah Spring Member in USW G-4, and the abundance of mordenite increases with depth throughout that unit. Only a trace of mordenite is seen in the same unit in the core from J-13 where it is below the water table. Mordenite is present in fractures in the zeolitic tuff of Calico Hills in J-13, as it is in USW G-4. In other zeolitic intervals below the water table in USW G-4, mordenite is also present. It appears that it may be stable as a fracture-lining mineral below the water table only in the presence of matrix zeolites.

The most striking difference between fracture linings in the Topopah Spring Member in J-13 and in USW G-4 is the presence of coarse-grained heulandite and near absence of euhedral quartz in USW G-4 and the absence of heulandite and abundance of drusy quartz in J-13. It is not known when the heulandite formed in fractures in the Topopah Spring Member at Yucca Mountain. Fine-grained mordenite was deposited in fractures in that unit after the lithophysal fractures were sealed. The coarse-grained heulandite and more mordenite were deposited later yet. Abundant slickensides suggest that the fine-grained mordenite was deposited before or during tectonic movement. The heulandite does not show evidence of abrasion suggesting that it may have been deposited after tectonic movement on those fractures had ceased. The elevation of the SWL is nearly the same for J-13 and USW G-4 (Robison, 1984); the stratigraphic difference in the SWL is a result of block faulting and tilting.

The most likely reason euhedral heulandite is not seen above the vitrophyre in J-13 is the fact that this interval, which is above the water table in USW G-4, is below the water table in J-13. Either the euhedral heulandite did not form in J-13 (possibly because this

interval was downfaulted to below the water table soon after the tuff cooled), or alternatively, heulandite was deposited in fractures but was destroyed when the interval became submerged. No relict heulandite was observed in J-13, but that may be attributed to the paucity of samples or to total dissolution of any that was deposited. In either case, it appears that heulandite is not stable under saturated conditions in nonzeolitic tuff. If that is true, then the presence of heulandite in fractures could be used to map the highest position of paleowater tables since the formation of the heulandite. Though ubiquitous, the quartz in J-13 is not in equilibrium at current conditions as it is etched and partially dissolved, though still euhedral. At least in one sample, the silica overgrowths appear to be cristobalite, but the identity of the silica overgrowths generally could not be determined.

Too little information is available about fracture coatings in the vitrophyre in the rest of Yucca Mountain to interpret the significance of the presence of chabazite in fractures in the vitrophyre in J-13.

VII. CONCLUSIONS

The presence of euhedral heulandite in fractures in devitrified tuffs may indicate unsaturated conditions since formation of the heulandite. The absence of heulandite and scarcity of mordenite in the densely welded tuff above the vitrophyre in J-13 suggest that, should that interval in the repository become saturated, the heulandite and perhaps much of the mordenite would be unstable and would be replaced by silica minerals. The zeolites in zeolitic intervals of the tuff should be preserved, as they are observed in those intervals in both USW G-4 and J-13 below the water table. A continuously cored hole that intersects the Topopah Spring Member below the water table is needed to verify these preliminary findings.

ACKNOWLEDGMENTS

Identification of chabazite in the XRD pattern from 1345 ft was made by S. Chipera. The author wishes to thank D. Broxton for critically reading this manuscript and suggesting improvements.

REFERENCES

Bish, D. L., D. T. Vaniman, F. M. Byers, Jr., and D. E. Broxton, "Summary of the Mineralogy-Petrology of Tuffs of Yucca Mountain and the Secondary-Phase Thermal Stability in Tuffs," Los Alamos National Laboratory report LA-9321-MS (November 1982).

Bish, D. L., and D. T. Vaniman, "Mineralogic Summary of Yucca Mountain, Nevada," Los Alamos National Laboratory report LA-10543-MS (October 1985).

Bish, D. L., and S. J. Chipera, "Mineralogy of Drill Holes J-13, UE-25A#1, and USW G-1 at Yucca Mountain, Nevada," Los Alamos National Laboratory report LA-10764-MS (September 1986).

Broxton, D. E., R. G. Warren, R. C. Hagan, and G. Luedemann, "Chemistry of Diagenetically Altered Tuffs at a Potential Nuclear Waste Repository, Yucca Mountain, Nye County, Nevada," Los Alamos National Laboratory report LA-10802-MS (October 1986).

Byers, F. M., Jr., and R. G. Warren, "Revised Volcanic Stratigraphy of Drill Hole J-13, Fortymile Wash, Nevada, Based on Petrographic Modes and Chemistry of Phenocrysts," Los Alamos National Laboratory report LA-9652-MS (January 1983).

Carlos, B. A., "Minerals in Fractures of the Unsaturated Zone from Drill Core USW G-4, Yucca Mountain, Nye County, Nevada," Los Alamos National Laboratory report LA-10415-MS (May 1985).

Carlos, B. A., "Minerals in Fractures of the Saturated Zone from Drill Core USW G-4, Yucca Mountain, Nye County, Nevada," Los Alamos National Laboratory report LA-10927-MS (April 1987).

Doyle, A. C., and G. L. Meyer, "Summary of Hydraulic Data and Abridged Lithologic Log of Ground-Water Test Well 6(J-13) Jackass Flats, Nevada Test Site, Nye County, Nevada," Technical Letter: NTS-50, prepared by the U.S. Geological Survey (USGS-474-314), for the U.S. Atomic Energy Commission (1963).

Heiken, G. H., and M. L. Bevier, "Petrology of Tuff Units from the J-13 Drill Site, Jackass Flats, Nevada," Los Alamos National Laboratory report LA-7563-MS (February 1979).

Robison, J. H., "Ground-Water Level Data and Preliminary Potentiometric-Surface Maps, Yucca Mountain and Vicinity, Nye County, Nevada," U.S. Geological Survey Water-Resources Investigations Report 84-4197 (1984).

Young, R. A., "Water Supply for the Nuclear Rocket Development Station at the U.S. Atomic Energy Commission's Nevada Test Site," U.S. Geological Survey Water-Supply Paper 1938, prepared in cooperation with the U.S. Atomic Energy Commission (1972).